URSI GASS 2020, Rome, Italy, 29 August - 5 September 2020

Computational Comparison of Power Density Definitions in the Proximity of Antennas for the Assessment of Human Exposure to EMF above 6 GHz

Kun Li(1), Kensuke Sasaki(2), Kanako Wake(2), Teruo Onishi(2), and Soichi Watanabe(2)
(1) Kagawa University, Takamatsu, Kagawa 761-0396, Japan
(2) National Institute of Information and Communications Technology, Koganei, Tokyo, 184-8795, Japan

Abstract

This study investigated the definition of power density for local exposure to electromagnetic fields (EMFs) by an antenna positioned near-by a human body at frequencies over 6 GHz. The relationship between the surface temperature elevation and the power densities in various near-field exposure conditions was analyzed . The results show that the applicability of the incident power density limits depends on the many factors, such as frequency, antenna, and antenna to body separation distance. Moreover, the analysis of heating factors of the absorbed power density demonstrated the dependence of locality of exposure. The findings obtained in this study may support the local exposure limits on the spatially-averaged power densities in safety guidelines and standard above 6 GHz.

1 Introduction

Rapid increase of using radio frequency (RF) transmitters in MMW bands has raised public concerns on human exposure to EMF in a general living environment [1] [2]. The use of MMW terminals in the vicinity of human body may result in a local temperature elevation on the skin surface due to the EMF exposure with a local beam.

Incident power density (*IPD*) is used as a metric in ICNIRP guidelines [3] and IEEE standard C95.1 [4] to protect human from excessive temperature elevation caused by EMF exposure. Recently, the draft of ICNIRP [5] and the revision of IEEE Std C95.1 [6] have been issued for human safety against MMW exposure, where the reference levels (RL) of *IPD* for local exposure are frequency-dependent values of $275f_G^{-0.177}$ and $55f_G^{-0.177}$ (f_G: frequency in GHz) from 6 to 300 GHz for occupational exposure/restricted environment and general public exposure/unrestricted environment [7] [8], respectively. In addition, the averaging area of 4 cm^2 between 6 and 30 GHz is suggested based on recent studies of thermal analysis [9] [10]. At frequencies higher than 30 GHz, averaging area may need to be reduced to consider the possibility of smaller beam sizes, such as 1 cm^2 (see Table 1). On the other hand, the power density inside a body surface has been mentioned as a new dosimetric limit for the basic restriction of local exposure, which is specified as the 'transmitted/absorbed power density (*APD*)' [5] [7] or 'epithelial power density' [6] [8]. Because the *APD* shows a high correlation with the surface temperature elevation, as confirmed by the recent studies [11] [12].

Table 1. Local exposure limits of incident power density from 6 to 300 GHz in recent safety guideline/standard.

IPD	f_G [GHz]	Ave. area [cm^2]	RL (General public)	RL (Occupational environment)
ICNIRP [5] [7]	6 – 30	4	$55f_G^{-0.177}$ W/m^2	$275f_G^{-0.177}$ W/m^2
	30 – 300	1		
IEEE [6]	6 – 300	4		

Although the amplitude of Poynting vector is generally used as the definition of power density in safety standard/guideline, detailed studies on the relationship between skin temperature elevation and physical quantities of each power density definition were not sufficiently reported. In particular, when radiation source is close to human tissue, due to the mutual interaction between antenna and body, the *IPD* in free space may not be suitable as a dosimetric measure for exposure level evaluation. As mentioned in the draft of ICNIRP [5], for the frequencies above 6 GHz, far-field reference levels are also applicable to radiative near-field exposure conditions, but no RL are provided for reactive near-field situation. On the basis of antenna theory, the boundary of the reactive near-field and the radiative near-field can be roughly determined from 8 to 0.16 mm at frequencies from 6 to 300 GHz ($\lambda/2\pi$, where λ is wavelength). However, for the compliance assessment of commercial wireless devices, as mentioned in the technical report by IEC [13], the minimum separation distance between the evaluation surface and the device for *IPD* is recommended to 2 mm. Due to the complexity of electromagnetic field distribution at a close distance from an antenna, power density definition should carefully be determined to prevent the possibility of underestimation of exposure level at frequencies over 6 GHz.

In this study, a computational comparison of power density definitions for MMW exposure have been conducted. Particular emphasis is placed on the relationship between surface temperature elevation and the incident, or absorbed power densities, in various near-field exposure conditions.

2 Model and Method

2.1 Configuration of human-skin model

Figure 1 shows a 4-layer skin model for dosimetry analysis, which is composed of epidermis, dermis, fat, and muscle, representing the skin tissue configuration in the forearm

[14]. The width of the skin model, i.e. w, and the thickness of each layer, i.e. l_i, are listed in Table 2. A half-wavelength dipole antenna is placed at a distance d from the skin surface from 6 to 300 GHz. The antenna input power is set to 10 mW. Although the dipole antenna in this frequency region is not used in practical, it is a typical electromagnetic source in computational simulation. The antenna was resonated with an adjusted length in order to reduce the impedance mismatch caused by the mutual interactions between antenna and skin tissue. The dielectric properties reported in [14] were used for comparison with the results in [11]. One-dimensional analysis to simulate the plane wave exposure was also conducted using the same skin model in Fig. 1.

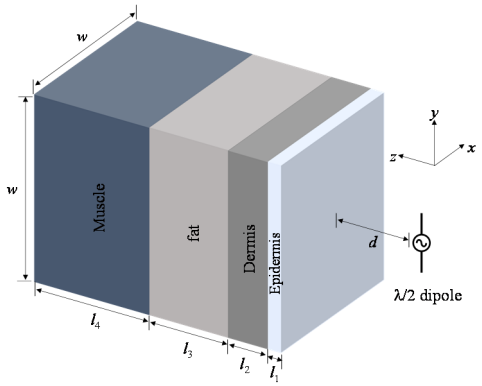

Figure 1. A three-dimensional four-layer skin model comprised of epidermis, dermis, fat, and muscle, and a half-wavelength dipole antenna.

Table 2. Dimension of 4-layer skin model in simulation

Parameters				
Model size	Frequency [GHz]			
	6-30	40-60	100	300
w [mm]	100	50	25	12.5
l_1 [mm]	0.2			
l_2 [mm]	1.0			
l_3 [mm]	3.8			
l_4 [mm]	15		5.0	
Resolution [mm]	0.2	0.1	0.05	0.025

2.2 Thermal parameters and bio-heat transfer computation

The finite-difference time-domain method (FDTD) [9] was used to analyze the electromagnetic fields both outside and inside the skin model. The SAR (specific absorption rate), representing the heat-generating source related to the electromagnetic wave exposure, is defined as

$$\mathrm{SAR}(\boldsymbol{r}) = \sigma(\boldsymbol{r})\frac{|\boldsymbol{E}(\boldsymbol{r})|^2}{2\rho(\boldsymbol{r})} \tag{1}$$

where $|\boldsymbol{E}(\boldsymbol{r})|$ is the electric field inside the skin tissue and $\boldsymbol{r}$ denotes the position vector. σ and ρ are the electrical conductivity and mass density, respectively. The temperature rise is obtained by solving Pennes's bio-heat transfer equation [15],

$$c(\boldsymbol{r})\rho(\boldsymbol{r})\frac{\partial T(\boldsymbol{r},t)}{\partial t} = \nabla\cdot\big(\kappa(\boldsymbol{r})\cdot\nabla T(\boldsymbol{r},t)\big) + \rho(\boldsymbol{r})\mathrm{SAR}(\boldsymbol{r}) + A(\boldsymbol{r},t) - B(\boldsymbol{r},t)\big(T(\boldsymbol{r},t) - T_b(\boldsymbol{r},t)\big) \tag{2}$$

where T and T_b are the temperatures of the human tissues and blood (°C), respectively. c is the specific heat and κ is the thermal conductivity. t is the time variable. A and B denote the basal metabolism per unit volume and a term associated with blood flow in each skin layer, respectively. The boundary condition for the heat exchange between the air and the skin tissue is given by

$$-\kappa(\boldsymbol{r})\frac{\partial T(\boldsymbol{r},t)}{\partial \boldsymbol{n}} = h\left(T_{surf}(\boldsymbol{r},t) - T_{air}(t)\right) \tag{3}$$

where h, T_{surf}, and T_{air} denote the heat transfer coefficient, surface temperature of the skin tissue, and air temperature, respectively, and $\boldsymbol{n}$ is the normal vector component to the boundary surface. The thermal parameters used in the temperature elevation analysis were set based on a previous study [16].

2.3 Incident and absorbed power densities

First of all, we discuss two general definitions of the *IPD* used by [9] and [13], respectively, as shown in the following equations,

$$Re[|\boldsymbol{S}_{tot}|] = \frac{1}{2A}\iint_A |Re(\boldsymbol{E}\times\boldsymbol{H}^*)|dA \tag{4}$$

$$Re[S_n] = \frac{1}{2A}\iint_A Re(\boldsymbol{E}\times\boldsymbol{H}^*)\cdot\boldsymbol{n}dA \tag{5}$$

where $\boldsymbol{S}_{tot}$ and S_n are the norm and normal component of a complex Poynting vector, respectively. $\boldsymbol{n}$ is the unit vector component normal to the model surface. A is the averaging area listed in Table 1. In this study, we also investigated the absorbed power density (*APD*), which has been studied by [11] [12], recently. It is verified that the *APD* crossing a unit area at air to skin boundary in the direction normal to the interface represents the total power absorbed by the skin tissue [11], defined as

$$APD = \frac{1}{2A}\iint_A Re\big(\boldsymbol{E}(\mathbf{r})\times\boldsymbol{H}^*(\mathbf{r})\big)\cdot\boldsymbol{n}dA\,|_{z=0} \tag{6}$$

where plus z-axis is perpendicular to the body surface, as the coordinate shown in Fig. 1. The *APD* also can be represented by the integral value of the SAR over the skin depth direction (see Eq. 2 in [12]). The same results of *APD* can be obtained using these two equations mathematically.

3 Results

Figure 2 shows the computational results of the heating factors, which are defined by the ratio of the peak surface temperature elevation in steady state (ΔT_{peak}) to *IPD*, as a function of frequency from 6 to 300 GHz. The λ/2 dipole antenna is set with a separation distance of d = 10 mm from

the skin surface. The results of plane wave incidence at normal direction were also included. Figs. 2 (a) and (b) indicate the heating factors when the averaging area A equals to 1 and 4 cm^2, respectively. As shown in Fig. 2 (a), when the averaging area A of 1 cm^2 is used, since the separation distance of d = 10 mm approaches the outside boundary of the radiative near-field region at 6 GHz (roughly at 8 mm), a small difference less than 7% between the use of norm and normal component of Poynting vector can be observed. Moreover, the heating factors of *IPD* shows below the heating factors of plane wave incidence situation. On the other hand, when A is increased to 4 cm^2, the variation between these two definitions of *IPD* is slightly increased to more than 15%. Compared with the case of plane wave incidence, the difference is within 37% at 6 GHz and no longer exceeds 15% above 10 GHz, indicating the frequency dependence of the averaged *IPD* over 6 GHz.

Figure 3 shows the ratio of the averaged *APD* to *IPD* using the λ/2 dipoles from 6 to 300 GHz. Here, the *IPD* defined as the normal component of Poynting vector (see Eq. 5) was used. The separation distance d was set to 2, 5, and 10 mm, respectively. As shown in Fig. 3, when d = 10 mm, the transmittances of dipoles show below that of the plane wave incidence except 6 GHz. When d is reduced to 2 mm, an obvious demarcation at 30 GHz can be observed. Especially at frequencies from 6 to 30 GHz, some results of transmittance exceed 1, which does not physically exist. This is because that a small separation distance such as 2 mm is almost covered by the near-field region of dipoles at the frequency below 30 GHz, where the effects caused by the mutual interaction between the antenna and the human body may be significant. In that case, the limit of using incident power density as a dosimetric measure is shown.

Figure 4 shows the heating factor of *APD* normalized to that of the dipole antenna at d = 10 mm as a function of separation distance d normalized to wavelength (λ). A half-wavelength dipole, the typical patch, 2x2, and 4x4 patch array antennas with in-phase feeding, were employed as the radiation sources. The frequency was set to 30 GHz. On the basis of the proposal in the draft of safety guideline [5], the averaging area of A = 4 cm^2 was utilized. As shown in Fig. 4, with the reduce of separation distance d from 10 to 2 mm, the heating factors of the *APD* using dipole and patch antenna are increased about 4.5 times. On the contrary, the results of 2x2 and 4x4 patch arrays do not change significantly. Especially for the case of 4x4 patch array antenna, an almost flat characteristic independent of separation distance as that of plane wave incidence in [11] is observed.

Figure 5 shows the normalized distributions of *APD* using different antennas at 30 GHz. The separation distance was d = 2 mm. In Fig. 5, compared with the results of the dipole and single patch antenna, which have sharp distributions around the position of peak values, the patch array antennas show relatively flat distributions of *APD* even the separation distance is 2 mm, corresponding to the results shown in Fig. 4. From these results, it was found that the locality of exposure caused by the radiation source may result in an increase of heating factor of the *APD*. However, considering the millimeter wave applications in practical, it may not be realistic to use such as single dipole or 1-element patch antenna in the actual devices.

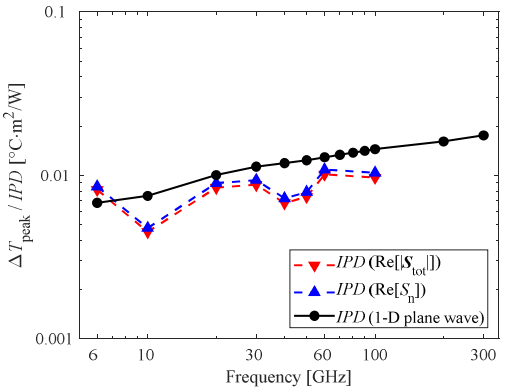

(a) A = 1 cm^2

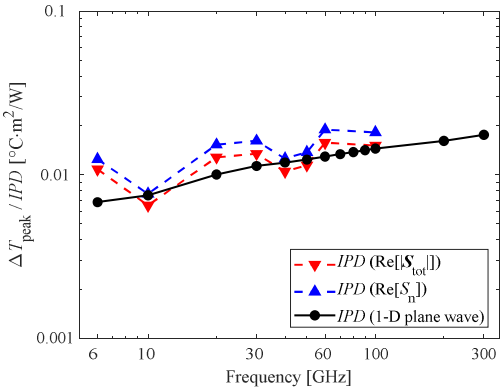

(b) A = 4 cm^2

Figure 2. Heating factor of using λ/2 dipoles with a separation distance of d = 10 mm when *IPD* were averaged over an area A of (a) 1 cm^2, (b) 4 cm^2.

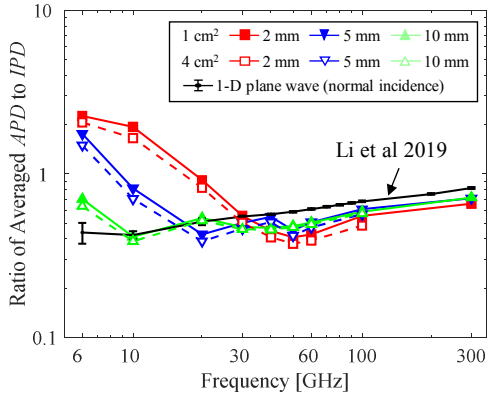

Figure 3. Ratio of averaged *APD* to *IPD* as a function of frequencies from 6 to 300 GHz using λ/2 dipole antennas with various separation distance.

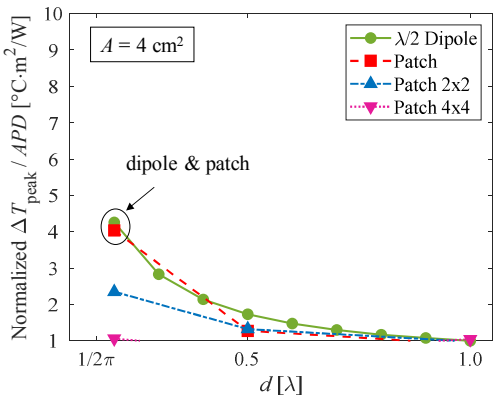

Figure 4. Normalized heating factor of *APD* when A = 4 cm^2 using different antennas at 30 GHz vs. normalized separation distance d.

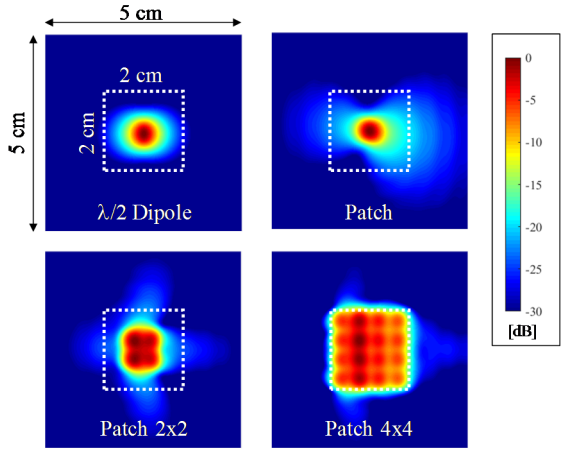

Figure 5. Normalized distributions of *APD* using different antennas at 30 GHz with a separation distance of d = 2 mm.

4 Conclusion

This study examined the comparison of power density definitions for EMF exposure assessment above 6 GHz. The relationship between the surface temperature elevation and the incident power density was firstly analyzed using the dipole antenna with various separation distances. The findings show the applicability of the *IPD* limits depends on the mutual interaction between the radiation source and human body, which is affected by frequency and separation distance. This is attributed to the complexity of antenna near-field property, which is essentially differentiated from the uniform exposure conditions in far-field, i.e. plane wave incidence. Moreover, the investigations of the heating factor of the *APD* demonstrated the importance of locality of exposure, which are valuable for discussing the local exposure limits on the spatially-averaged power density in safety guidelines/standard above 6 GHz.

5 Acknowledgements

A part of this work conducted by NICT was supported by the Ministry of Internal Affairs and Communications, Japan.

6 References

[1] M. Zhadobov, et al., "Millimeter-wave interactions with the human body: state of knowledge and recent advances," Int. J. Microwave Wireless Technol., vol. 3, no. 2, pp. 237-247, Mar. 2011.

[2] D. Colombi, et al., "Implications of EMF exposure limits on output power levels for 5G devices above 6 GHz," IEEE Antennas Wirel. Propag. Lett., vol. 14, pp. 1247–1249, 2015.

[3] "Guidelines for limiting exposure to time-varying electric, magnetic, and electromagnetic fields (up to 300 GHz)", Health Phys., vol. 74, pp. 494-522, 1998.

[4] IEEE Standard for Safety Levels with Respect to Human Exposure to the Radio Frequency Electromagnetic Fields, 3 kHz to 300 GHz, IEEE Std., C95.1, 2005.

[5] Draft of ICNIRP, "Guidelines for limiting exposure to time-varying electric, magnetic, and electromagnetic fields (100 kHz to 300 GHz)", 2018.

[6] IEEE Standard for Safety Levels with Respect to Human Exposure to Electric, Magnetic, and Electromagnetic Fields, 0 Hz to 300 GHz, IEEE Std., C95.1, 2019.

[7] A. Hirata, "Review of dosimetry studies for setting the ICNIRP Guidelines", BioEM2019, Session W2-3, Montpelier, France, Jun. 2019.

[8] C. K. Chou, et al., "Revision of IEEE Standards C95.1–2005 and C95.6–2002", Proc. BioEM2018, Slovenia, pp. 326–31, 2018.

[9] Y. Hashimoto, et al., "On the averaging area for incident power density for human exposure limits at frequencies over 6 GHz," Phys. Med. Biol., vol. 62, no. 8, pp. 3124-3138, 2017.

[10] K. R. Foster, et al., "Thermal modeling for the next generation of radiofrequency exposure limits: commentary", Health Phys. vol. 113, pp. 41–53, 2017.

[11] K. Li, et al., "Relationship between power density and surface temperature elevation for human skin exposure to electromagnetic waves with oblique incidence angle from 6 GHz to 1 THz," Phys. Med. Biol., vol. 64, no. 6, pp. 065016, Mar. 2019.

[12] D. Funahashi et al., "Area-Averaged Transmitted Power Density at Skin Surface as Metric to Estimate Surface Temperature Elevation", IEEE Access, vol. 6, pp. 77665 – 77674, Dec. 2018.

[13] Measurement procedure for the evaluation of power density related to human exposure to radio frequency fields from wireless communication devices operating between 6 GHz and 100 GHz, document IEC TR63170, 2018.

[14] K. Sasaki, et al., "Monte Carlo simulations of skin exposure to electromagnetic field from 10 GHz to 1 THz," Phys. Med. Biol., vol. 62, pp. 6993–7010, 2017.

[15] A. Hirata, et al., "Temperature elevation in the eye of anatomically based human head models for plane-wave exposure," Phys. Med. Biol., vol. 52, pp. 6389–99, 2007